AAEC/E 112

AAEC/E 112

AUSTRALIAN ATOMIC ENERGY COMMISSION

RESEARCH ESTABLISHMENT

LUCAS HEIGHTS

THE IRRADIATION BEHAVIOUR OF HOT-PRESSED DISPERSIONS OF (U, Th)Be_{13} IN BERYLLIUM

– SECOND IRRADIATION EXPERIMENT

by

G. L. HANNA

B. S. HICKMAN

R. J. HILDITCH

Issued Sydney, November 1963

UNCLASSIFIED

AUSTRALIAN ATOMIC ENERGY COMMISSION

RESEARCH ESTABLISHMENT

LUCAS HEIGHTS

THE IRRADIATION BEHAVIOUR OF HOT-PRESSED DISPERSIONS OF (U, Th)Be_{13} IN BERYLLIUM

- SECOND IRRADIATION EXPERIMENT

by

G. L. HANNA

B. S. HICKMAN

R. J. HILDITCH

ABSTRACT

Fuel specimens having uranium-thorium beryllides as the fissile bearing phase were irradiated at 400 to 700°C to burn-ups between 7 and 11 a/o uranium in a predominantly thermal flux.

Two specimens of massive (U,Th)Be_{13} exhibited good dimensional stability and low fission gas release. Dispersion specimens containing 20, 35, and 50 v/o (U,Th)Be_{13} swelled by 3 to 18 per cent. and released up to 33 per cent. of the gaseous fission products.

The results indicate that the mixed beryllide is an inherently good fuel material and lead to the conclusion that the poor irradiation stability of hot-pressed specimens may not be typical of (U,Th)Be_{13}-Be dispersions prepared by other techniques.

CONTENTS

1. INTRODUCTION

A fuel system of possible application in high–temperature reactors is a dispersion of mixed beryllides of uranium and thorium in a beryllium matrix. An irradiation experiment aimed at studying the contribution of fission fragment damage in this system was described previously by the authors (Hanna, Hickman, and Hilditch, 1962). In rig X–11, hot–pressed cylinders were irradiated in a thermal neutron flux at temperatures between 430° and 530°C. These temperatures were 100 – 200°C below the operating temperature envisaged for high temperature reactor systems. In a second experiment, using rig X–70, specimen temperatures of 500 – 700°C were achieved.

The results of the X–11 experiment were not encouraging and led to the expectation that the irradiation behaviour of hot–pressed material at least, would not permit its use at 600 – 700°C. Fission gas releases were between 0.3 and 1.8 per cent. and volume increases between 0.4 and 5 per cent; these values were considered to be too great in view of the relatively low temperatures.

Materials and fabrication techniques were the same in both experiments. Beryllide contents and fission densities were similar and the only differences of major significance were the higher irradiation temperatures and the inclusion of specimens of massive $(U,Th)Be_{13}$ in the X–70 experiment.

2. EXPERIMENTAL

2.1 Specimen Compositions

The variables studied in this experiment were beryllide content, fuel particle size, and fission density. Although specimen temperatures varied over a range of 200 °C there was no control over this variation (see Section 2.4).

Details of specimen compositions and fuel particle size are given in Table 1. Specimens were divided into seven groups of four but only the first two of each group were irradiated. The third of each group was used as a heat–treatment control to indicate thermal effects, which were independent of irradiation, and the fourth as an "as–fabricated" control.

Specimens 33–36 were rectangular prisms of uranium–thorium beryllide and specimens 41–64 were cylindrical compacts of beryllides dispersed in beryllium. The fissile:fertile ratio was nominally 1 U : 2 Th in all specimens except one set of dispersions (numbered 57–60) which contained no thorium.

The beryllide contents of dispersions were 20, 35, and 50 volume per cent. The beryllide particle size which was common to the three compositions was 100 – 150 microns. Specimens 53 – 56 contained 35 volume per cent. of 0 – 50 micron particles and specimens 61 – 64, 50 volume per cent. of 150 – 300 micron particles. Specimens 57 – 60 in which no thorium was used contained 35 volume per cent. of 100 – 150 micron particles.

Chemical analysis of the beryllides (see Table 2) showed the UBe_{13} to be stoichiometric and the $(U,Th)Be_{13}$ to be slightly hyperstoichiometric and to have a U : Th ratio of 1:2.3. X–ray diffraction demonstrated that the $(U,Th)Be_{13}$ was a solid solution but that the solution was not homogeneous.

2.2 Specimen Preparation

Specimen fabrication and irradiation techniques were the same as used in the X–11 experiment; details were given by Hanna, Hickman, and Hildtich (1962) and Hanna, Turner, and Smith (1961). Briefly, beryllide fuel material was prepared by reaction–hot–pressing the mixed metal powders at 1550°C and 1 t.s.i. for 60 minutes under an argon atmosphere. Prisms for irradiation were obtained by cutting the compacts with a diamond slitting wheel and particles for dispersion specimens were prepared by crushing and sieving. The fine, minus 50 micron powder was obtained by repeated grinding of minus 300 mesh powder.

Dispersion specimens were prepared by a double vacuum hot–pressing of beryllide–beryllium powder mixtures, the compacts being inverted between pressings. The compacts were machined on a lathe to their final dimensions of 0.75 and 0.9 cm diameter by 2 cm long.

2.3 Pre-irradiation Examination

The dimensions and densities of all specimens (see Tables 6 and 7) were measured before irradiation. Dimensions were measured with a vernier micrometer to an accuracy of 0.00025 cm. Densities were determined by weighing in air and in n-octyl alcohol after thorough impregnation.

Metallographic examination was done on samples of the beryllide powders and optical particle size measurements were made on particles mounted on a glass slide.

The following points summarise the as-fabricated condition of the specimens:

(i) Densities of dispersion specimens were below the theoretical densities and decreased as the volume fraction of fuel phase increased. Average apparent densities were:

for 20 v/o dispersoid 98 per cent. T.D.

35 v/o dispersoid 94 per cent. T.D.

50 v/o dispersoid 89 per cent. T.D.

(ii) The beryllide prisms (specimens 33 – 36) were grey in colour, suggesting that they were porous. Porosity could not be measured as chips at corners and edges prevented accurate volumes being determined from dimensions. Displacement densities were 94.5 to 96 per cent. of theoretical.

(iii) Fuel particles were mostly plate- or needle-shaped. The majority were porous but the number of pores varied from particle to particle.

(iv) Chemical analyses of the beryllides (Table 2) revealed that the $U Be_{13}$ was stoichiometric and that the $(U,Th)Be_{13}$ contained a slight excess of beryllium and had a U : Th ratio of 1:2.3.

2.4 Irradiation

Specimens were irradiated in the 4V-1 hole in HIFAR using a standard A.A.E.C. four-inch fuel rig. They were arranged in two side-by-side stringers each of which carried seven specimens. Duplicate specimens were placed in corresponding positions in each stringer so that they would be exposed to similar neutron fluxes during irradiation. The stringer containing specimens having odd identification numbers was referred to as stringer A and that containing specimens having even numbers as stringer B. The only source of heat was the nuclear heating of the specimens themselves, and heat transfer across a helium-filled gap of pre-determined dimensions gave the desired specimen temperature.

On the first approach to power the temperature of specimen 58 rose to 825 °C at a power level of 8 MW and that of specimen 57 would have exceeded 800 °C at 10 MW. As 800 °C had been set as the maximum operating temperature the rig was withdrawn from the pile and surrounded with a stainless steel sleeve of a thickness (0.162 in) calculated to reduce the temperatures to an acceptable level. On the second approach to power the highest specimen temperature (number 58) was 725 °C at 10 MW.

Specimen temperatures rose gradually during irradiation and the temperature of specimen 58 eventually exceeded 800 °C after about 500 hours. At this stage, temperatures of all specimens in stringer B were reduced a little by rotating the rig so that stringer A acted as a shield. The temperature rise continued, however, and was eventually traced to a leakage of air into the helium occupying the free space of the rig. Irradiation was continued with periodic purging of the rig with helium. A temperature drop of about 20 °C was observed in the hottest specimens at each purge.

The irradiation temperatures of individual specimens are given in Figures 1a and 1b and time-weighted mean temperatures in Table 3. The values quoted are the lower thermocouple temperatures which, in general, were higher than those indicated by the upper couples.

At each reactor start–up, transient temperature peaks occurred in which temperatures rose to 10 – 30 °C above the subsequent steady operating temperatures.

The actual irradiation time was 3400 hours. During the irradiation there were fourteen reactor trips of 1 to 3 hours and five shut–downs of several days.

2.4 Post–irradiation Examination

The amounts of fission product gases released from the specimens during irradiation were measured by piercing the inner cans in an evacuated system of known volume and measuring the pressure rise. Gas compositions were determined by mass–spectrometry. Cans were raised to 150 °C during sampling to melt the sodium and release any entrapped gas. All specimens except number 46 were successfully sampled. The specimens were than removed from the cans, washed in alcohol to remove the sodium, and stored under alcohol until the density measurements were made.

Specimen surfaces were examined and photographed at magnifications of 2 to 15 times using a stereo–periscope. Dimensions were measured with a micrometer and densities determined by weighing in air and in n–octyl alcohol after impregnation under reduced pressure. Transverse and longitudinal metallographic sections were prepared from each specimen irradiated in stringer A. Control samples taken from specimen 44 (as–fabricated condition) and specimen 43 (unirradiated, heat–treated condition) were prepared with the irradiated samples. Specimens were etched for about 20 seconds in a solution of 2½ per cent. hydrofluoric acid, 5 per cent. nitric acid in absolute alcohol.

The burn–up in each specimen was calculated from tabulated flux data obtained during low power operation of HIFAR (Connolly and McKenzie 1960) and from integrated fluxes determined from gamma spectrometry of cobalt monitors. Flux depression in each specimen was estimated by the empirical method described by Lewis (1955).

Specimens numbered 46 and 61 were analysed for burn–up by radio–chemical determination of the Cs – 137 yield.

2.5 Out–of–Pile Control Specimens

One specimen of each group defined in Table 1 was given a heat treatment which followed closely the thermal history of the hotter of its two kindred specimens in the irradiation rig. The specimens received the same post–treatment examinations as the irradiated specimens.

3. RESULTS

3.1 Burn–Up

The results of burn–up determinations are given in Table 4. In calculating burn–ups from tabulated fluxes, allowance was made for the stainless steel sleeve used to lower the specimen temperatures. Nevertheless, these estimates are greater than the burn–ups obtained from cobalt monitor activities. The values obtained from Cs – 137 determinations agree well with those for the cobalt monitors, and give confidence in the latter results.

The burn–ups in stringer B specimens were consistently lower than those in stringer A specimens. This reflects the radial orientation of the rig and the shielding of stringer B by stringer A. Burn–ups were between 7.2 and 11.2 a/o U in stringer A and between 6.1 and 9.3 a/o U in stringer B. The corresponding fission densities are given in Table 4.

3.2 Fission Product Gas Release

The quantities of gaseous fission products released from the specimens are shown in Table 5. These are quoted as actual volumes of each stable isotope found in each can and as percentages of the total amount of each isotope produced in the specimen. The latter figures were calculated using burn–up values determined from gamma spectrometry of the cobalt monitors.

The percentage releases from the $(U,Th)Be_{13}$ prisms and the most dilute dispersions (20 v/o $(U,Th)Be_{13}$) were less than 0.5 per cent. Specimens containing 30 v/o fuel phase released from 0.5 to 8.4 per cent. of the gases at about 3×10^{20} fission cm^{-3} and 25 per cent. of the gases at 1.9×10^{20} fission cm^{-3}.

The releases from specimens 53 and 54, containing fine fuel grains, were 0.5 and 4.0 per cent. which are lower than those from specimens 45 and 46, containing 100-micron fuel grains and the same volume-fraction of fuel. This contrasts with releases from specimens containing 50 per cent. fuel phase; those containing 250-micron fuel grains (numbers 61 and 62) released only 1 per cent. of the gases and those containing 100-micron grains (numbers 45 and 46) released about 10 per cent.

Releases as high as 25 and 22 per cent. were measured for specimens 57 and 58 respectively. These specimens contained 35 v/o of UBe_{13} and were irradiated to fission densities of 1.9 and 1.6×10^{21} fissions cm^{-3} respectively. The reasons for these high gas releases became apparent during the metallographic examination and are discussed in Sections 3.6 and 4.

3.3 Macroexamination

With the exception of specimens 33 and 34 ($(U,Th)Be_{13}$) and 53 and 54 (dispersions) all specimens suffered considerable surface roughening during irradiation. Several had swollen and of these some were bent or barrelled and had cracked transversely. Typical surface conditions are illustrated in Figure 2. Specimen 33 had broken into two pieces when recovered from the irradiation can.

The surface condition of specimens 57 and 58 was different to that of other specimens in that the surface was extremely rough and consisted of an array of rounded particles (Figure 3a). Sectioning specimen 57 for metallographic preparation revealed a distinct band (Figure 3b) around the specimen. Even in the as-sectioned condition this band appeared to have a columnar structure. The inside diameter of the shell corresponded very closely to the original specimen diameter.

Unirradiated heat-treated control specimens suffered only very slight surface change; surfaces were still smooth but had become grey in colour.

With both the irradiated and heat-treated control specimens storage in alcohol (see Section 2.4) resulted in the precipitation of a white powder. This powder was extremely soluble in water and contained a small amount of beryllium (as shown by rough spectrographic analysis). The X-ray diffraction pattern was complex and could not be interpreted from the A.S.T.M. X-ray data cards.

3.4 Dimension and Density Measurements

Dimensional changes on irradiation are listed in Table 6. Results of density measurements are not quoted as specimen porosity prevented reliable determinations.

Except for specimens 57 and 58, all dispersion specimens showed smaller diametral increases (between about 1 per cent. and 4 per cent.) than longitudinal increases (from 1.5 to 11 per cent.). Volume increases were from 3 to 18 per cent.

Specimens 57 and 58 increased by about 0.3 cm in both diameter and length which represents more than 30 per cent. increase in diameter and 80 per cent. in volume; metallographic examination indicated the reason for this uniform increase in dimensions (see Section 3.5).

Dimensional increases in the pure beryllide specimens 33 and 34 were between 0.16 and 0.75 per cent. and there was no preferential direction for expansion.

Dimension changes in heat-treated control specimens are given in Table 7. Specimen 35 ($(U,Th)Be_{13}$) increased by 0.7 and 0.8 per cent. along its minor axes and by only 0.08 per cent. along its major axis. Dispersion specimens increased by 0.1 to 1.5 per cent. in diameter and 0.35 to 4.7 per cent. in length. All longitudinal increases were greater than diametral increases.

3.5 Metallographic Examination

The microstructure of the irradiated $(U,Th)Be_{13}$ specimen numbered 33 was cleaner and less porous than that of the as-fabricated control specimen 36 (see Figure 5). The irradiated specimen showed a non-uniform distribution of irregularly shaped pores and occasional areas of very fine spots. Examination at a magnification of 600 times suggested that some of these spots were holes whilst

others were a foreign phase which could not be identified. Owing to its poor condition, similar areas could not be positively identified in the control sample. However, they have been observed in other as-fabricated specimens (Hanna and Turner 1963).

The irradiated specimen responded much more readily to the etchant than did the unirradiated specimen and etching showed that the grain structure was not altered by irradiation. Apart from the difference in etching behaviour, no effect was observed which could be directly attributed to irradiation. The greater porosity in the unirradiated specimen is considered to be due to variations in the compact from which they were prepared and not to sintering during irradiation.

The microstructures of all dispersion specimens showed similar features which were more pronounced in specimens of high fuel content. These are illustrated in Figures 6b to 11b. The most striking feature was the long intergranular cavities in the beryllium matrix. These were evident to a small degree with 20 v/o fuel (Figure 6b) and were very pronounced with 35 and 50 v/o fuel (Figures 7b and 8b). In specimen 53, containing small fuel particles, the cavities were again evident but were noticeably shorter (Figure 9b).

Fragmentation of fuel grains also occurred in several specimens, varying in extent from occasional large cracks as in Figure 11b to severe fragmentation along grain boundaries as in Figure 7b. Large irregular cavities frequently occurred adjacent to fuel particles and were probably due to the loss of fragments during polishing.

Heat-treated unirradiated control specimens also showed the tendency to form cavities at the beryllium grain boundaries. However, fractures in the fuel particles were confined to occasional large cracks such as were found in the as-fabricated condition.

The microstructure of specimen 57 (Figure 10) was striking in that all the beryllium – originally the matrix – lay in a shell around the specimen surface. Practically no beryllium could be found in the specimen interior. Inside the shell of beryllium, the fuel particles formed a continuous network whose diameter corresponded closely to the original diameter of the dispersion compact. Considerable fragmentation of the fuel grains had occurred (see Figure 10b).

The outer shell of beryllium had a columnar appearance but grains were equiaxed and about 200 microns across (Figure 4). (The original grain size in the hot-pressed compacts was about 50 microns). The structure strongly suggested that the beryllium had been ejected in the liquid state from the body of the specimen.

4. DISCUSSION

The behaviour of specimens irradiated in this experiment was inferior to that of specimens in the X-11 experiment (Hanna et al. 1962). A comparison of dimensional changes and fission gas releases in the two experiments is made in Figures 12 and 13 using fuel content as the basis for comparison. These graphs show that both dimension changes and fission gas releases were significantly higher in this experiment than would be predicted by interpolation from the results of X-11 experiment.

Metallography showed that the swelling in dispersion specimens was largely due to the formation of cavities at the grain boundaries in the beryllium matrix. Pore formation at the fuel particle surfaces, as was observed in the X-11 experiment, probably occurred, but the importance of this contribution was obscured by fragmentation of fuel particles and probable loss of fragments during polishing.

The results show an apparent tendency for volume expansion to increase with the amount of porosity in the unirradiated specimens. However, as porosity was closely related to the volume fraction of fuel phase, the most porous specimens were also those in which total fission gas yields were highest.

One would expect pores to act as reservoirs where the pressure of fission gases could build up and cause swelling. Unfortunately, the true distribution of pores in the unirradiated specimens was obscured by probable tear-out of fuel particle fragments during metallographic preparation.

Consequently it was not clear whether the appearance of cavities at the beryllium grain boundaries was directly due to the agglomeration of fission gases in existing pores or whether they resulted from stresses imposed by the pressure of fission gases in larger pores adjacent to fuel particles.

The fractional releases of fission gases from dispersions of 35 and 50 volume per cent. $(U,Th)Be_{13}$ were similar in magnitude to the theoretical fractional losses from the fuel particles. This implies that all gas recoiling to the matrix was able to leave the specimens and, presumably, the escape occurs in the later stages of swelling when pores become interconnected.

The same fabrication procedures were used to prepare specimens for both this and the X–11 experiment. There is no reason, then, why the inferior behaviour in this case should have been due to differences in specimen quality. If it was due to differences in irradiation conditions the responsible factors must have been differences in neutron flux, temperature, and burn–up. Because of the lower neutron flux (and hence fission rate) used in this experiment the irradiation time was forty per cent. greater than in the X–11 experiment. Thus, although specimen temperatures and burn–ups were only slightly higher, the three factors together would have led to higher gas losses (if due to diffusion–dependent processes) and to higher swellings.

Melting of the beryllium in specimens 57 and 58 is not explained by the temperature records which, from experience in similar rigs containing uranium specimens, are considered to be in error by no more than 75 °C. The highest temperatures recorded were 745 °C for specimen 57 and 850 °C for specimen 58. Melting without an indicated temperature rise would have required formation of a film of either sodium vapour or fission gases on the specimen surface. Under steady–state conditions, film boiling of the sodium would not have occurred until a temperature of 1080 °C. Thus film boiling could only have led to melting if a very sudden temperature excursion occurred; there is no reason to suppose that this did in fact take place.

Calculation shows that a surface film of fission gas only eleven microns thick would have raised the temperature of specimens 57 and 58 to about 1300 °C without altering the sodium temperature. This represents a film volume at N.T.P. of only 0.00034 cm^3 compared with the measured release of about 0.5 cm^3. The formation of such a film therefore seems feasible and offers the most plausible explanation of matrix melting. It should be pointed out however, that all other specimens released more gas than required to form an insulating film of the required thickness. Of these, only specimen 54 showed any sign of matrix melting and this was confined to one end–face only. Why the melting should have been confined to specimens 57 and 58 is not obvious but may be associated with the higher temperatures of these specimens and a more uniform distribution of gas bubbles over the specimen surface. The formation of a uniform shell of beryllium around the specimen suggests that the melting occurred late in the irradiation when the pressure of fission gases in the matrix was great enough to force the metal to the outside.

Dimensional stabilities and fission gas retentions of specimens having different fuel particle sizes did not follow the trends predicted by dispersion fuel theory. Specimens 61 and 62 (250–micron fuel particles) underwent similar dimension changes to specimens 49 and 50 (100–micron particles) but released only about one–tenth as much of the fission gases. Specimens 53 and 56, containing 10–micron fuel particles, exhibited much lower dimension changes and gas releases than specimens 45 and 46, which contained 100–micron particles.

The good irradiation behaviour of the $(U,Th)Be_{13}$ specimens (numbered 33 and 34) and the unchanged nature of fuel particles in most dispersions indicates that the beryllides are an inherently good fuel material. This supports the conclusion (Hanna, Hickman, Hilditch 1962) that some unknown factor associated with the fabrication of dispersion specimens is the probable cause of their poor behaviour. Clare and Silver (unpublished) have shown the feasibility of extruding small specimens containing up to 30 volume per cent. of $(U,Th)Be_{13}$ and any future experiments should explore the possibility that extruded specimens will behave more favourably than hot–pressed ones.

5. CONCLUSIONS

The results of this experiment are consistent with those from the earlier one in rig X–11 in showing that the dimensional stability and fission gas retention of $(U,Th)Be_{13}$–Be specimens prepared by hot–pressing are poor. However, the behaviour in this experiment was generally less favourable.

Volume changes derived from dimensions were always greater than 3 per cent, and in some specimens were as high as 18 per cent. Fission gas releases were generally high and in one set of specimens reached about 25 per cent.

The cause of the swelling has not been elucidated; the swelling, rather than being the direct result of irradiation, may derive from inadequacies of the hot-pressing procedure used for specimen fabrication. Before the results are taken as being typical of the (U,Th)Be_{13}–Be system, a further experiment using extruded specimens should be done.

6. ACKNOWLEDGMENTS

The authors are indebted to the following for assistance in the execution of the experiment: members of Operations Division for assembly and operation of the rig, Analytical Chemistry Section for fission gas and burn-up analyses, and, in particular, the Hot Cells Group for the post-irradiation examination.

7. REFERENCES

Connolly, J.W., and McKenzie, C.D. (1960). – AAEC/TM64.

Hanna, G.L., Hickman, B.S., and Hilditch, R.J. (1962). – AAEC/E96.

Hanna, G.L., Turner, D.N., and Smith, P.D. (1961). – AAEC/TM113.

Hanna, G.L., and Turner, D.N. (1963). – AAEC/E102.

Lewis, W.B. (1955). – Nucleonics 12 (10): 31.

TABLE 1

DETAILS OF SPECIMENS

Specimen Number	Volume Per cent. Fuel	Atom Ratio U : Th	Fuel Particle Size, (microns)
33 – 36	100	1 : 2	–
41 – 44	20	1 : 2	100
45 – 48	35	1 : 2	100
49 – 52	50	1 : 2	100
53 – 56	35	1 : 2	10
57 – 60	35	1 : 0	100
61 – 64	50	1 : 2	250

TABLE 2

ANALYSIS OF INTERMETALLIC COMPOUNDS

Substance	w/o U	w/o Th	w/o Be	BeO w/o	Atom Ratio U : Th : Be
$U Be_{13}$	62.5	–	32.5	3.7	1 : 0 : 13
$U Th Be_{13}$	19.7	44.3	33.8	2.0	1 : 2.3 : 436 ($M Be_{13.2}$)

TABLE 3

IRRADIATION TEMPERATURES

Specimen	Temperature Range °C	Mean Temperature °C
33	510 – 640	555
34	510 – 630	525
41	450 – 600	555
42	500 – 660	550
45	350 – 500	395
46	495 – 670	555
49	520 – 640	580
50	440 – 600	505
53	520 – 650	580
54	415 – 620	460
57	600 – 745	650
58	620 – 850	695
61	520 – 635	565
62	490 – 600	545

TABLE 4

BURN–UP IN IRRADIATED SPECIMENS

Specimen No.	Tabulated Flux Data		Co Monitored Fluxes			Cs – 137 Yield	
	a/o U	a/o Heavy Metals	a/o U	a/o Heavy Metals	Fission Density (fissions cm^{-3} of specimen)	a/o U	a/o Heavy Metals
33	8.8	2.9	7.9	2.6	6.4×10^{20}		
34	9.1	3.0	7.3	2.4	5.9×10^{20}		
41	12.2	4.7	10.7	3.6	1.8×10^{20}		
42			9.3	3.1	1.6×10^{20}		
45	11.5	3.8	11.2	3.7	3.2×10^{20}		
46			9.1	3.0	2.6×10^{20}	9.5	3.2
49	9.7	3.2	8.4	2.8	3.5×10^{20}		
50			8.2	2.7	3.4×10^{20}		
53	11.4	3.8	10.9	3.6	3.1×10^{20}		
54			8.8	2.9	2.5×10^{20}		
57	8.9	8.9	7.2	7.2	1.9×10^{21}		
58			6.1	6.1	1.6×10^{21}		
61	8.9	3.0	7.5	2.5	3.1×10^{20}		
62			–	–		7.1	2.4

TABLE 5

FISSION GAS RELEASES

Specimen No.	Volume of Gas (cm^3)							Per cent. Release							Mean
	Krypton			Xenon				Krypton			Xenon				
	83	84	86	131	132	134	136	83	84	86	131	132	134	136	
	x 10^{-5}	x 10^{-5}	x 10^{-5}	x 10^{-5}	x 10^{-5}	x 10^{-5}	x 10^{-5}								
33	4	8	16	30	46	86	118	0.3	0.3	0.3	0.35	0.5	0.5	0.7	0.4
34	4	8	16	28	43	79	109	0.3	0.35	0.35	0.4	0.4	0.4	0.7	0.4
41	7	12	25	48	74	127	177	0.6	0.55	0.6	0.75	0.75	0.7	1.2	0.65
42	6	12	24	45	67	115	158	0.5	0.6	0.6	0.75	0.8	0.7	1.2	0.6
45	157	310	590	950	1480	2700	8870	7.1	7.6	7.2	7.7	8.2	8.2	14.5	8.6
46	–	–	–	–	–	–	–								
49	211	407	781	1250	1991	3542	4990	8.8	9.2	8.9	9.5	10.3	10.1	17.5	10.7
50	264	505	952	1580	2450	4470	6175	11.5	11.8	11.1	12.2	13.0	13.0	22.1	13.5
53	10	19	36	64	95	164	225	0.5	0.5	0.5	0.5	0.5	0.5	0.9	0.55
54	79	150	280	524	760	1325	1825	4.6	4.7	4.3	5.4	5.4	5.1	8.6	5.4
57	700	1330	2560	4000	6220	11270	15710	26.9	27.7	26.9	28.0	29.6	29.5	50.7	31.3
58	630	1200	2300	3580	5580	10180	13900	28.6	29.2	28.0	29.1	31.0	31.0	52.2	32.7
61	22.8	44	84	136	214	389	536	1.1	1.1	1.1	1.2	1.2	1.25	2.1	1.3
62	20.3	39	75	122	192	347	477	1.0	1.0	1.0	1.1	1.2	1.15	2.0	1.2

TABLE 6

DIMENSION CHANGES IN IRRADIATED SPECIMENS

Specimen	Pre-irradiation Density % Theoretical	Diameter (cm)			Length (cm)			Change in Volume %
		Before	After	% Change	Before	After	% Change	
33	94.5	0.577 *	0.581	0.7	1.257	Broken	–	–
		0.615	0.622	0.75				
34	96.0	0.596 *	0.5975	0.16	1.256	1.262	0.5	1.14
		0.568	0.570	0.30				
41	96.1	0.901	0.909	0.9	2.006	2.040	1.7	3.5
42	97.0	0.899	0.908	1.0	2.017	2.051	1.8	3.8
45	95.5	0.901	0.930	3.1	2.035	2.143	5.3	11.5
46	96.3	0.895	0.908	1.4	2.040	2.093	2.6	5.4
49	93.3	0.896	0.935	4.3	2.147	2.305	7.3	15.9
50	92.6	0.895	0.925	3.4	2.138	2.375	11.1	17.9
53	96.3	0.896	0.906	1.1	2.027	2.065	1.8	4.0
54	95.5	0.895	0.901	0.7	2.055	2.087	1.5	2.9
57	96.7	0.895	1.213	35	2.078	2.426	16.8	86.8
58	96.7	0.896	1.185	32	2.076	2.419	16.5	80.5
61	92.6	0.897	0.930	3.5	2.130	2.363	10.9	17.9
62	92.3	0.898	0.934	2.8	2.155	–	–	–

* Square Section

TABLE 7

DIMENSION CHANGES IN HEAT–TREATED CONTROL SPECIMENS

Specimen No.	Pre–treatment Density % Theoretical	Irradiated Specimen	Diameter (cm)			Length (cm)			Change in Volume %
			Before	After	% Change	Before	After	% Change	
35	96	33	0.608 *	0.613	0.8	1.254	1.255	0.08	1.7
			0.643	0.648	0.7				
43	98.7	41	0.901	0.903	0.2	1.993	2.001	0.35	0.75
47	94.8	45	0.902	0.908	0.6	2.052	2.067	0.7	1.9
51	93.3	49	0.899	0.900	0.1	2.130	2.161	1.45	1.6
55	95.2	53	0.897	0.899	0.2	2.077	2.090	0.6	1.0
59	95.2	58	0.899	0.913	1.5	2.100	2.198	4.7	7.7
63	91.6	61	0.899	0.904	0.5	2.158	2.206	2.2	3.2

* Square Section

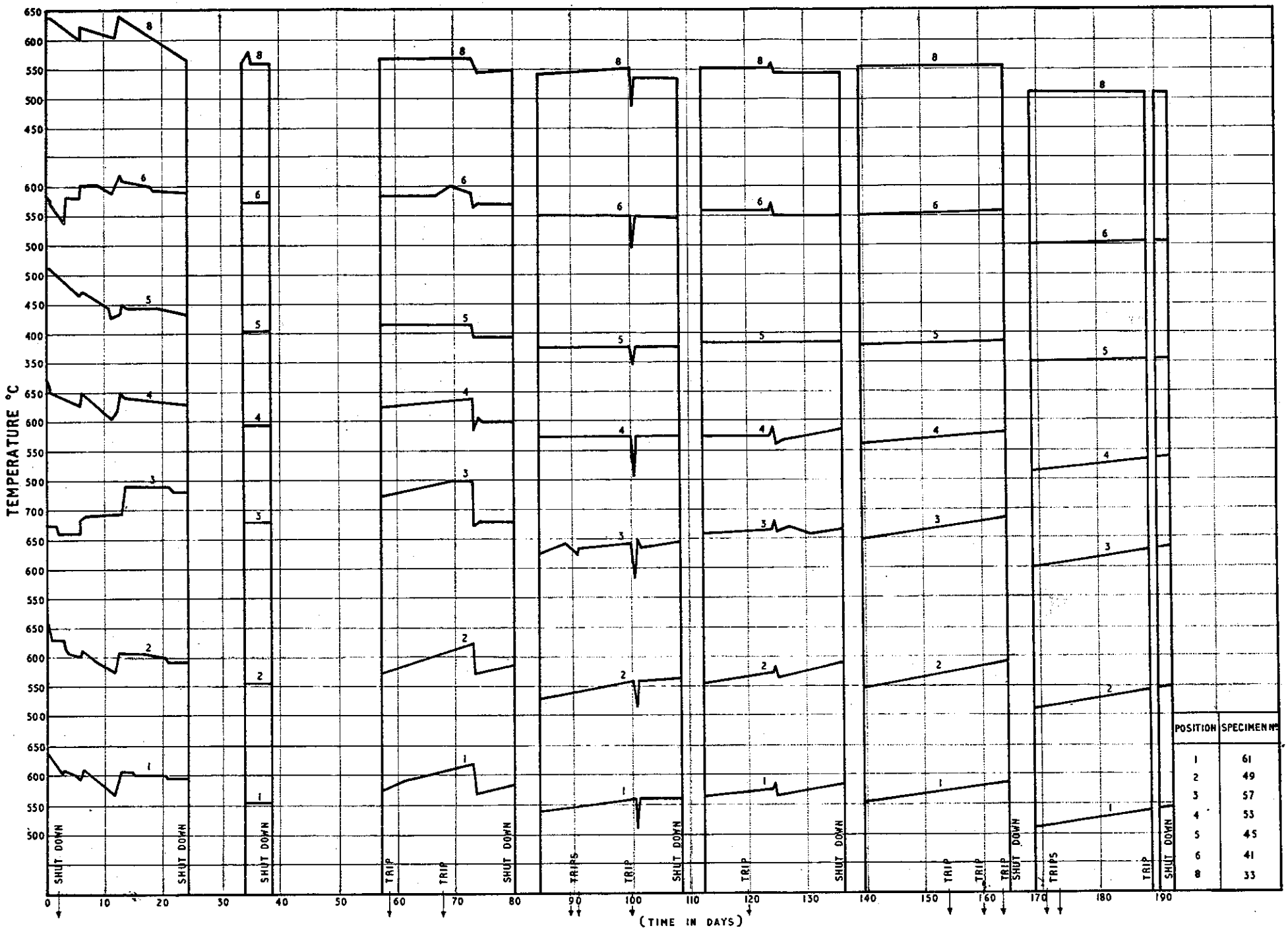

FIGURE 1a X-70 TEMPERATURE CHART — STRINGER A

P 396

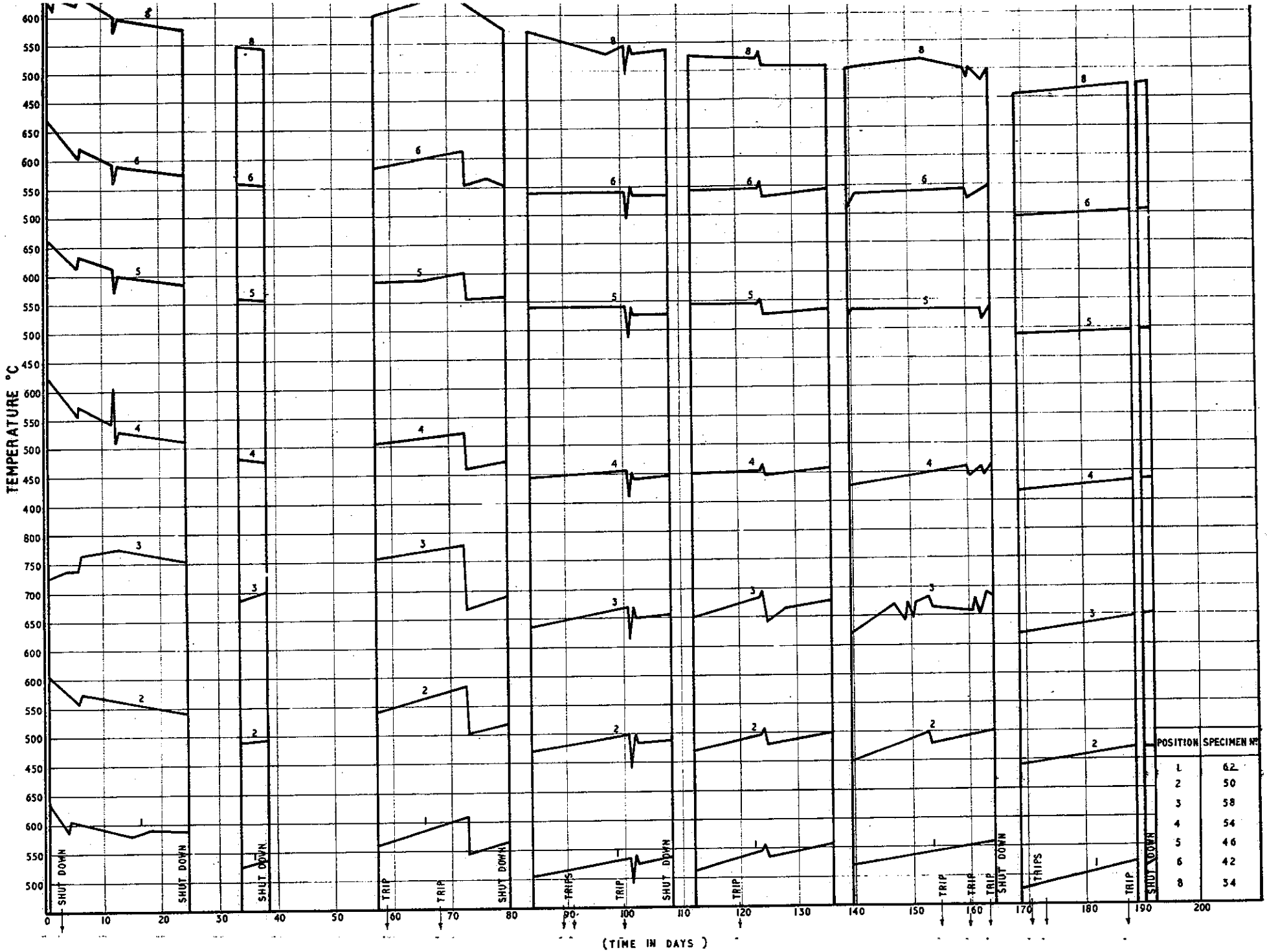

FIGURE 4b X-70 TEMPERATURE CHART —— STRINGER B

A396

X 4

(a) Specimen 49

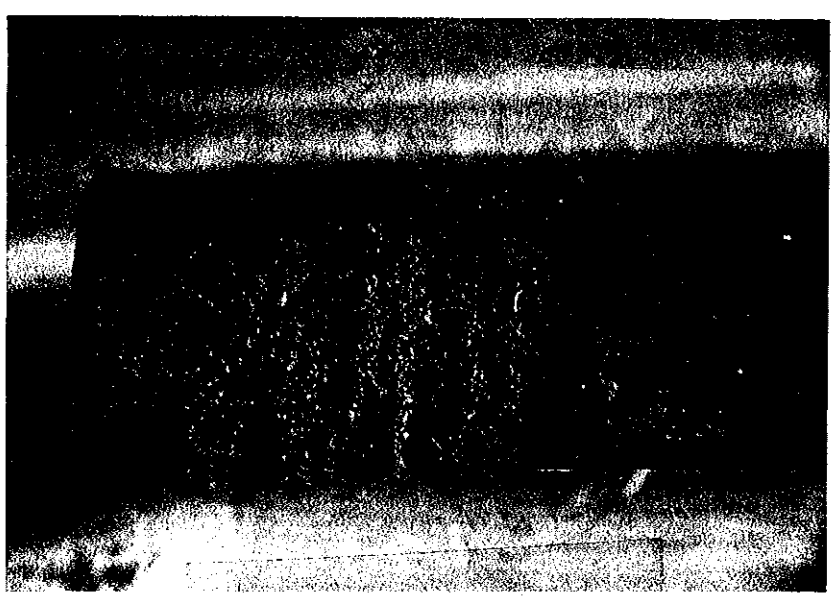

X 4

(b) Specimen 61

FIGURE 2 APPEARANCE OF TYPICAL SPECIMENS AFTER IRRADIATION

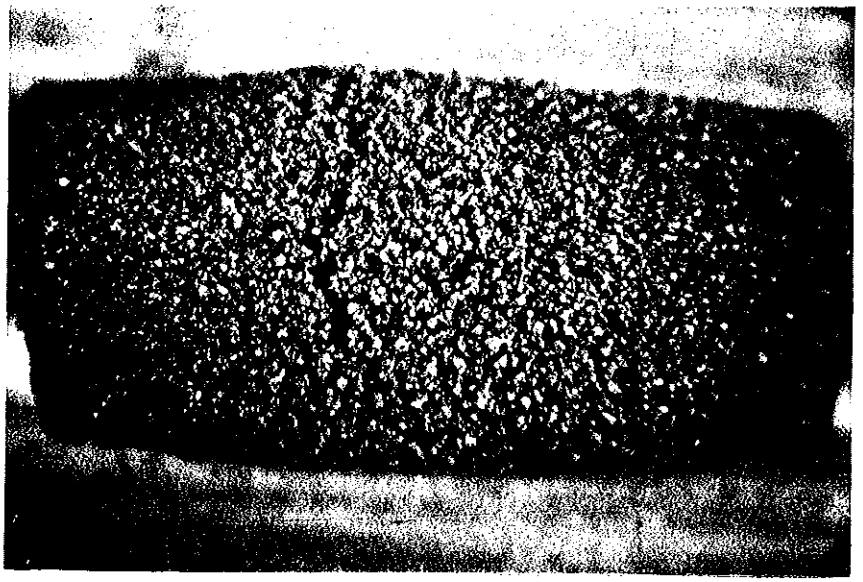

X 4

FIGURE 3a SPECIMEN 57 AFTER IRRADIATION

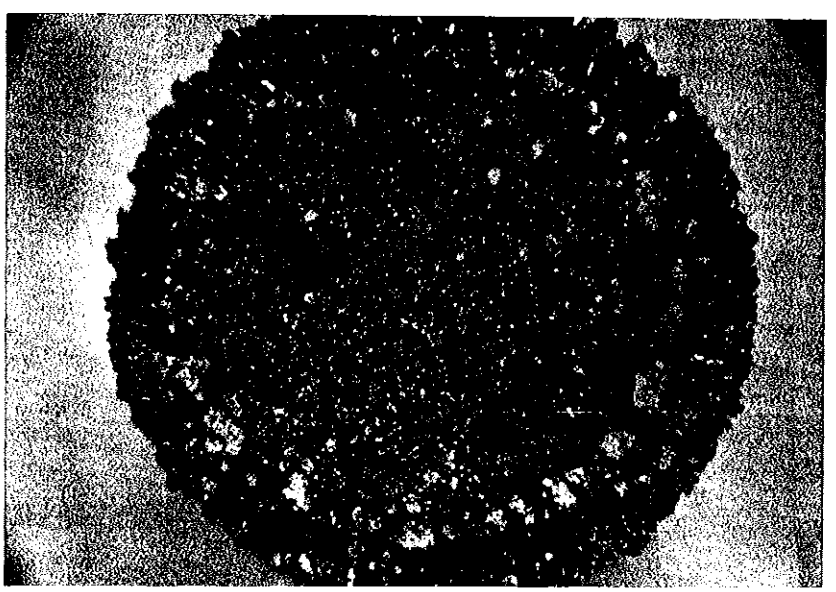

X 7

FIGURE 3b CROSS SECTION OF SPECIMEN 57 AFTER SLITTING

X 48

FIGURE 4 PHOTOMICROGRAPH OF BERYLLIUM SHELL AROUND SPECIMEN 57

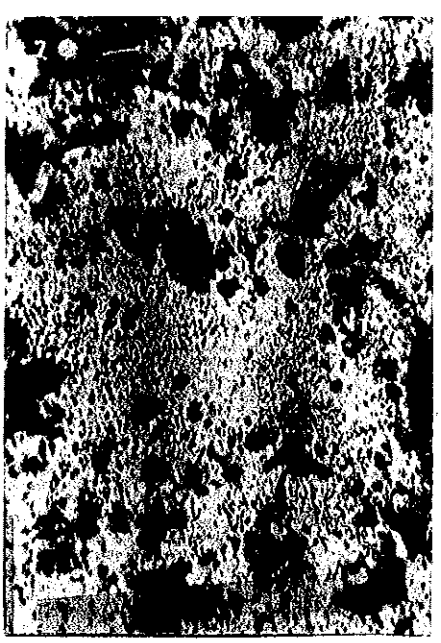

X 160

(a) Unirradiated

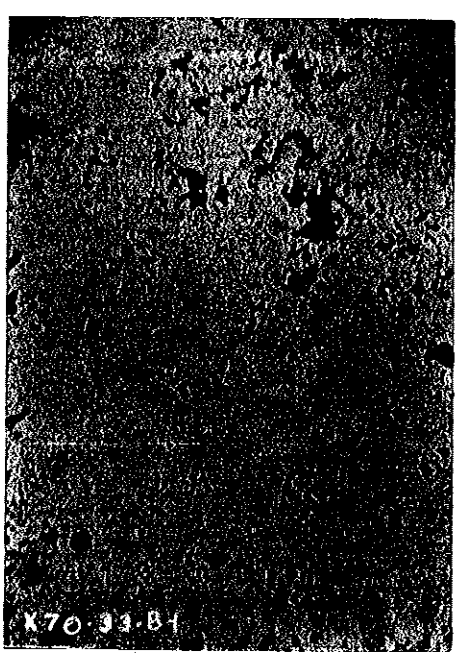

(b) Irradiated

X 160

FIGURE 5 MICROSTRUCTURE OF SPECIMENS 33-36

X 160

(a) Unirradiated

X 160

(b) Irradiated

FIGURE 6 MICROSTRUCTURE OF SPECIMENS 41-44

X160

(a) Unirradiated

X160

(b) Irradiated

FIGURE 7 MICROSTRUCTURE OF SPECIMENS 45-48

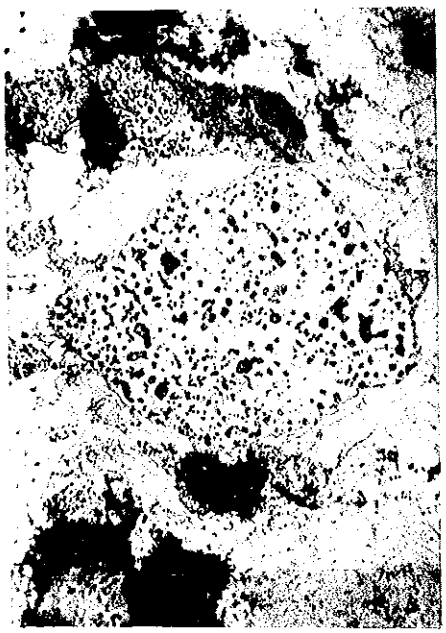

X 160

(a) Unirradiated

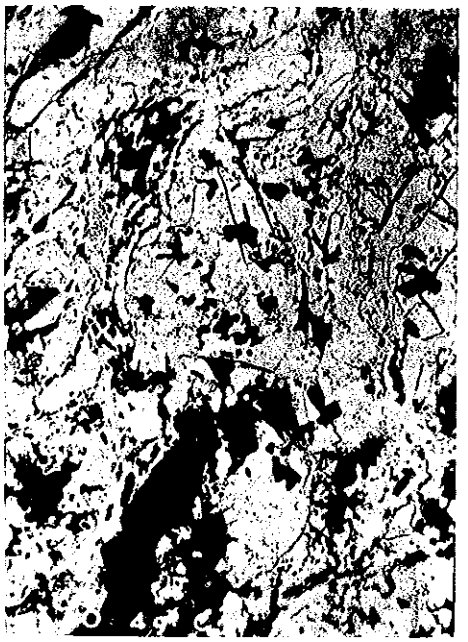

X 160

(b) Irradiated

FIGURE 8 MICROSTRUCTURE OF SPECIMENS 49-52

X 160

(a) Unirradiated

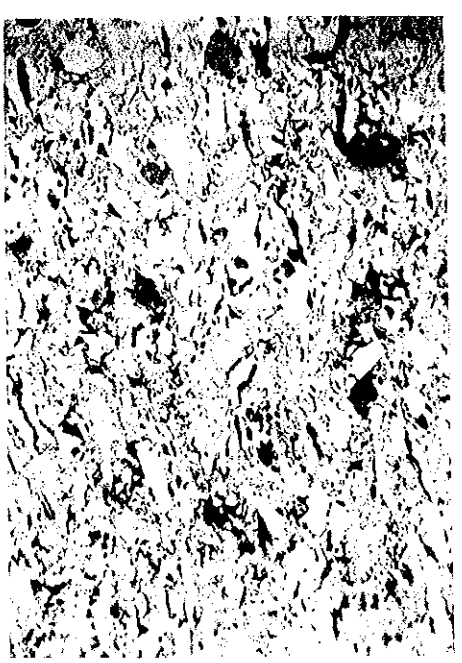

X 160

(b) Irradiated

FIGURE 9 MICROSTRUCTURE OF SPECIMENS 53-56

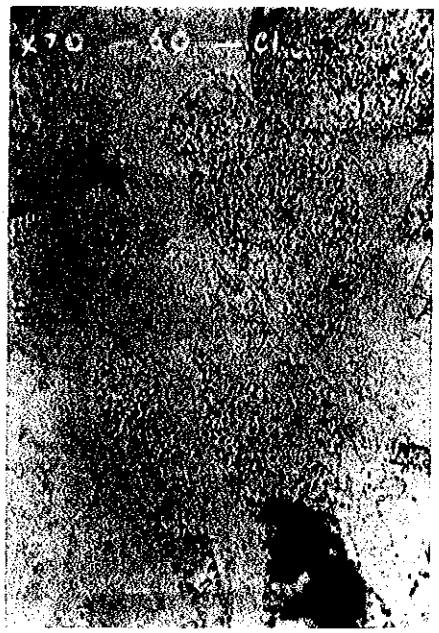

X160

(a) Unirradiated

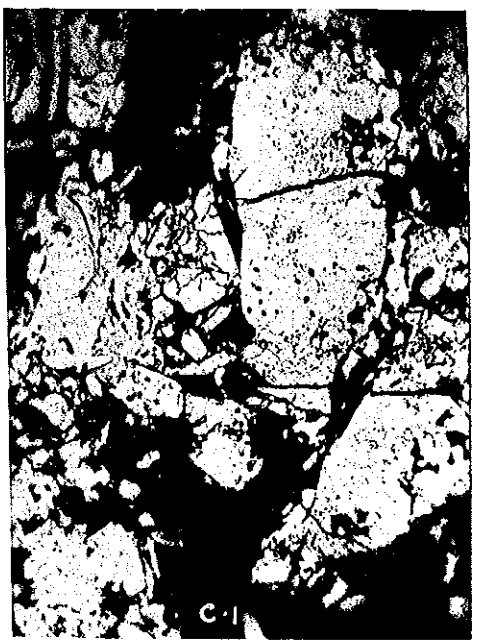

X160

(b) Irradiated

FIGURE 10 MICROSTRUCTURE OF SPECIMENS 57-60

X 160

(a) Unirradiated

X 160

(b) Irradiated

FIGURE 11 MICROSTRUCTURE OF SPECIMENS 61-64

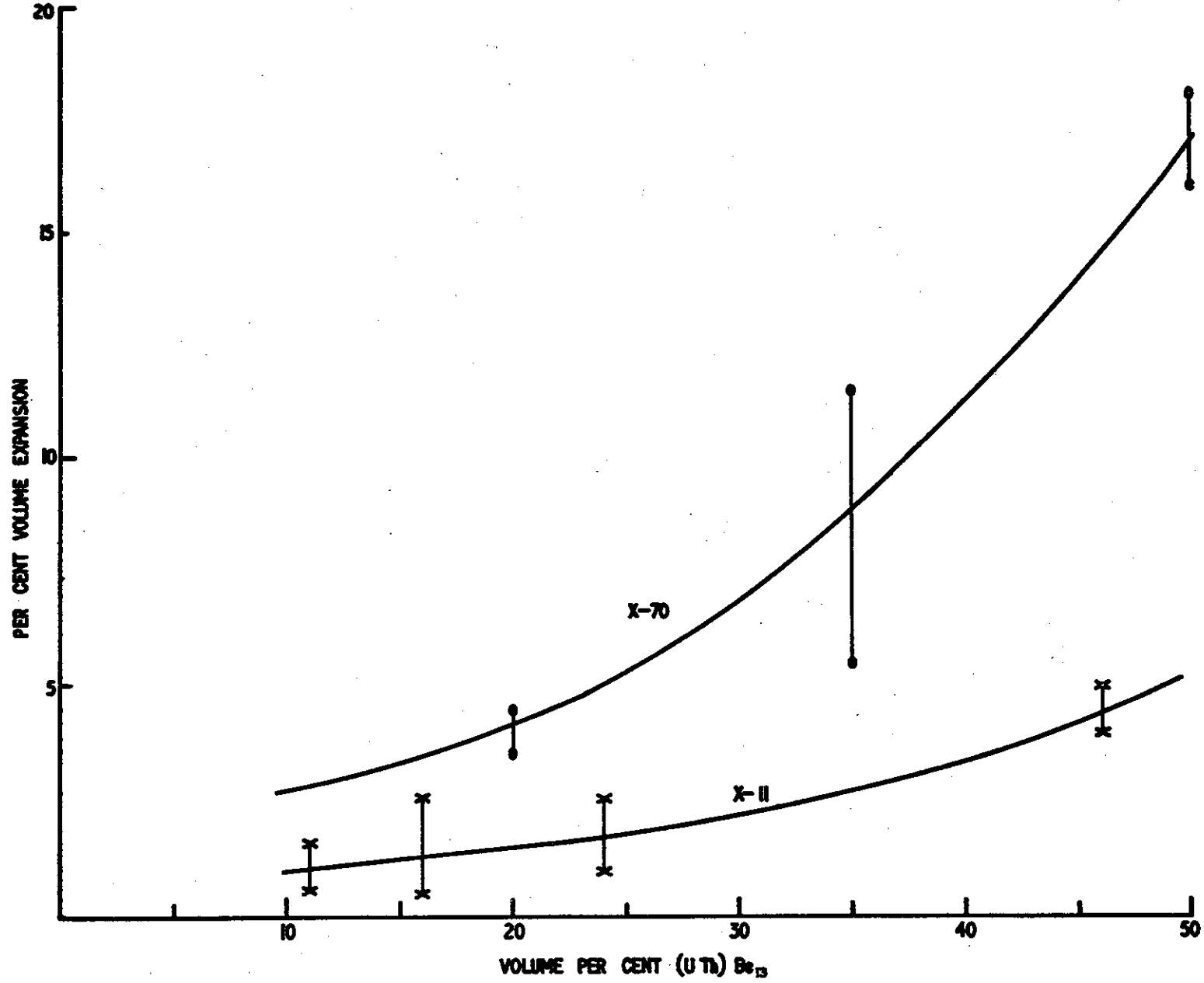

FIGURE 12

COMPARISON OF DIMENSION CHANGES IN X-II AND X-70 EXPERIMENTS

P413

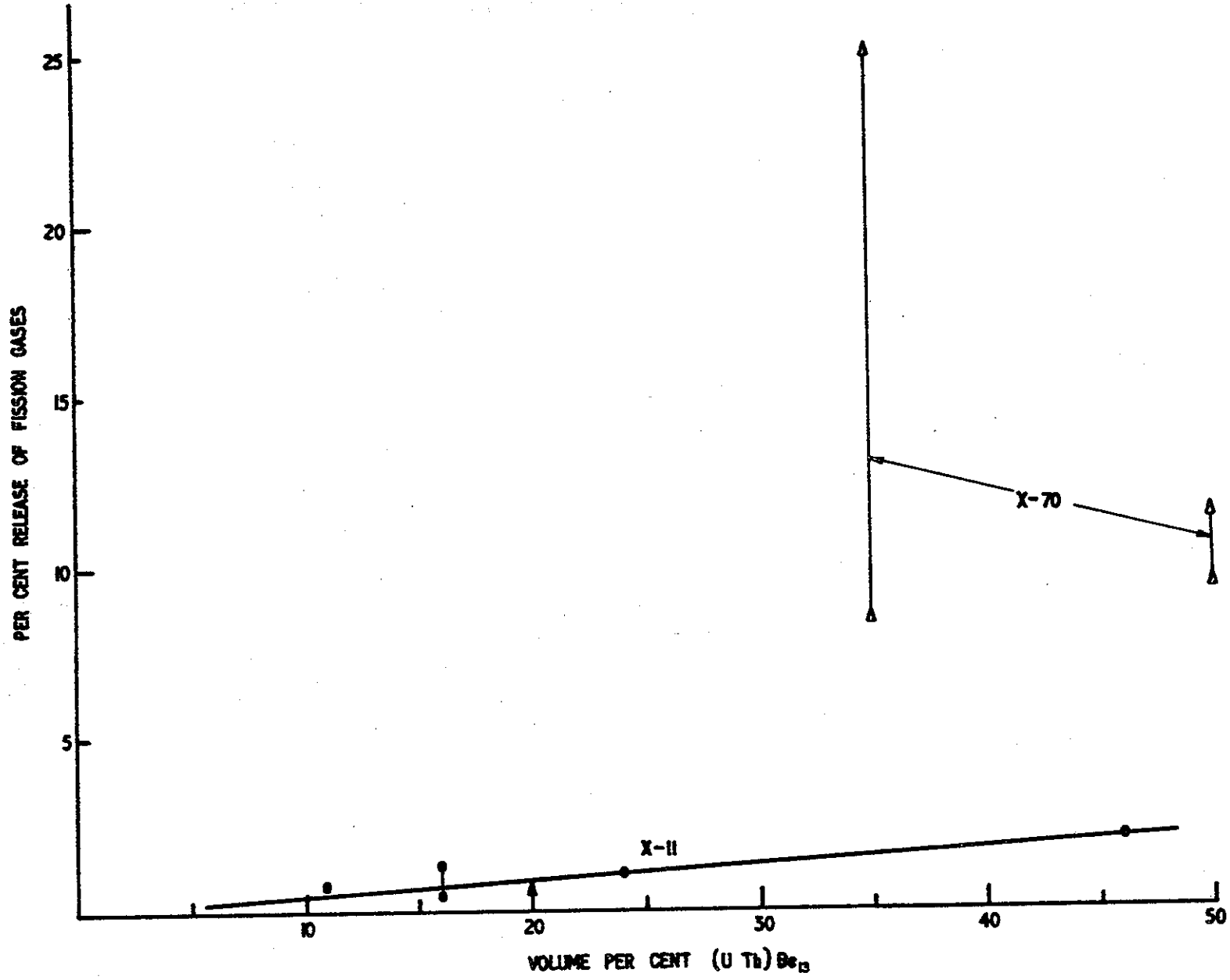

FIGURE 13
COMPARISON OF FISSION GAS RELEASES IN X-11 AND X-70 EXPERIMENTS P413